

Biomarker reconstruction of the early Eocene paleotopography and paleoclimate of the northern Sierra Nevada

Michael T. Hren¹, Mark Pagani¹, Diane M. Erwin², and Mark Brandon¹

¹Department of Geology and Geophysics, Yale University, New Haven, Connecticut 06511, USA

²Berkeley Museum of Paleontology, Berkeley, California 94720, USA

ABSTRACT

We reconstruct ancient temperature and elevation gradients across the early Eocene (52–49 Ma) northern Sierra Nevada (California, United States) using organic molecular proxies that record atmospheric and ground-level effects of topography. Paleoelevation was determined by reconstructing the change in the hydrogen isotopic composition of precipitation ($\Delta\delta D_{\text{precip}}$) and mean annual temperature (ΔT_{GDGT}) (glycerol dialkyl glycerol tetraethers) from the isotopic composition of fossil angiosperm leaf *n*-alkanes and the distribution of microbially produced soil tetraethers preserved in leaf-bearing sediments. Organic molecular data produce equivalent range-scale ($\delta D_{n\text{-alkane}}$) and channel (T_{GDGT}) paleoelevation estimates that show the northern Sierra Nevada was a warm (>6–8 °C warmer than modern), high-elevation (>2 km), and moderate- to low-relief landscape at the Eocene Climatic Optimum. Modern northern Sierra Nevada topography likely reflects post-Paleocene reduction of mean surface elevation and late Cenozoic increases in relief.

INTRODUCTION

The timing of major surface uplift of the Sierra Nevada (California, United States) remains a highly contentious issue that fundamentally affects our understanding of the role of tectonic and climatic processes in shaping topography. In general, there are two views of the evolution of the Sierra Nevada. The first is based on westward-tilting Miocene basalt flows preserved in paleochannels along the west flank of the mountain range, and argues that the Sierra Nevada reached modern mean elevations in the late Cenozoic through 1.5–2.5 km of surface uplift (Huber, 1981; Unruh, 1991; Wakabayashi and Sawyer, 2001) in response to removal of dense mantle lithosphere in the southern Sierra Nevada (Ducea and Saleeby, 1998; Saleeby et al., 2003; Jones et al., 2004; Zandt et al., 2004) and isostatic response to increased erosion resulting from late Cenozoic climate change (Small and Anderson, 1995). A second view argues that the Sierra Nevada achieved high elevations by the Late Cretaceous–early Cenozoic, forming the edge of a high continental plateau (Garside et al., 2005; Mulch et al., 2006; Cassel et al., 2009), and that modern topography resulted from slow post-Paleocene surface lowering and late Cenozoic changes in relief (House et al., 1998; Cecil et al., 2006). Stable isotope data support the presence of a high Eocene mountain range (Mulch et al., 2006) with minimal late Cenozoic change in range elevations (Poage and Chamberlain, 2002; Mulch et al., 2008; Crowley et al., 2008; Cassel et al., 2009). However, there remains considerable uncertainty over the timing of surface uplift and long-term changes in range relief.

Fluvial channels in the northern Sierra Nevada provide a unique opportunity to study both the

evolution of tilting and development of paleotopography in one setting. Our contribution builds on the work of Mulch et al. (2006) and Cassel et al. (2009) by using organic molecular temperature proxies and compound-specific stable isotope measurements of ancient leaf mats to reconstruct climatic and topographic gradients across the northern Sierra Nevada. Our study extends the work of Mulch et al. (2006) in sampling a larger distance across the mountain range, and obtaining well-constrained early Eocene (52–49 Ma) organic geochemical data that record range-scale and channel paleoelevations and provide an indication of early Sierra Nevada relief.

PALEOCHANNEL SEDIMENTS

Eocene–Oligocene sediments composed of clay, sand, and conglomerate fill paleochannels on the west flank of the Sierra Nevada from near sea level to >2000 m (Lindgren, 1911; MacGinitie, 1941). Within the lowermost bench gravels, abundant plant fossils are preserved within floodplain sediments and in-filled river meanders along the major Tertiary drainages. Plant fossils are classified as Chalk Bluffs Flora after their best-preserved occurrence, and are dated at 52–49 Ma by faunal and floral correlation (MacGinitie, 1941; Wing and Greenwood, 1993). Paleochannel gravels overlying leaf-bearing sediments are highly weathered and provide key evidence for high Eocene elevations (Mulch et al., 2006).

PALEOTOPOGRAPHY RECONSTRUCTION

The isotopic composition of precipitation and ground-level temperature reflect elevation at the range and local scales. The hydrogen iso-

topic composition of precipitation, δD_{precip} , is a function of equilibrium fractionation between atmospheric water vapor, precipitation, and the degree of rainout from an airmass during orographic ascent (Rowley et al., 2001; Poage and Chamberlain, 2001), and is predominantly controlled by surface elevation in mountainous regions. In the Sierra Nevada, δD_{precip} values decrease by 50‰ between the west and east sides of the mountain range (Ingraham and Taylor, 1991). Air temperature decreases with elevation due to adiabatic cooling of a rising airmass. Local temperature lapse rates are dependent upon sea-level temperature and moisture content, but globally average 5.5 °C/km (Meyer, 2007). Differences between range-scale (δD_{precip}) and ground-level (T , °C) paleoelevation proxies record elevation information on different spatial scales and can thus provide an indication of relief.

Recent advances in organic geochemistry have introduced new methods for estimating paleotemperature and the isotopic composition of local waters that can be directly related to elevation. In modern soils, the degree of methylation and cyclization of microbially derived branched glycerol dialkyl glycerol tetraethers (GDGTs) are related to mean annual temperature and pH, and provide a reliable indication of ancient temperature (Weijers et al., 2007a, 2007b). Similarly, long-carbon chain *n*-alkanes produced on the surface of higher plant leaves record the hydrogen isotope composition of precipitation (δD_{precip}), and can be preserved in sedimentary rocks with no isotopic exchange over geologic time (Schimmelmann et al., 1999). Here we examine organic molecular records of ancient surface temperature (T_{GDGT}) and $\delta D_{n\text{-alkane}}$ preserved in ca. 50 Ma Chalk Bluffs flora sediments to reconstruct climate and elevation gradients across the northern Sierra Nevada during the Eocene Climatic Optimum.

METHODS

We quantify early Eocene Sierra region topography by measuring: (1) the hydrogen isotope composition of odd-carbon numbered, high-molecular-weight *n*-alkanes (nC_{29} and nC_{31}) and (2) changes in paleo-mean annual temperature (MAT, °C) of fossil leaf localities using the recently established soil tetraether temperature proxy (Weijers et al., 2007a). Leaf-wax and tetraether compounds were extracted

from cuticle-rich sedimentary leaf mats at 17 Chalk Bluffs paleofloral sites in the northern Sierra Nevada (Fig. 1) and analyzed for δD and GDGT compound distributions (see the GSA Data Repository¹).

RESULTS AND DISCUSSION

The apparent isotope fractionation between precipitation and leaf-wax $\delta D_{n\text{-alkane}}$ ($\epsilon_{\text{apparent}}$) depends on soil-water evaporation, evapotranspiration, leaf morphology, and plant type (Chikaraishi and Naraoka, 2003; Smith and Freeman, 2006). Although the magnitude of apparent fractionation in leaf waxes can vary between species or leaves of one plant due to different rates of evapotranspiration, at high relative humidities, $\epsilon_{\text{apparent}}$ from plants of similar classes (i.e., angiosperms) is relatively constant (Sachse et al., 2006; Hou et al., 2008). These conditions are satisfied for Sierra Nevada paleochannel environments, as Chalk Bluffs flora indicate a humid, angiosperm-dominated subtropical forest with little to no grasses or gymnosperms (MacGinitie, 1941; Wing and Greenwood, 1993). Accordingly, we assume a constant $\epsilon_{\text{apparent}}$. Ultimately, our paleoelevation reconstruction does not require a priori knowledge of the magnitude of biosynthetic fractionation or the degree of isotopic enrichment due to evapotranspiration, only that $\epsilon_{\text{apparent}}$ is relatively constant across the terrain.

Our results show that $\delta D_{n\text{-alkane}}$ values systematically decrease with distance from the Eocene shoreline (Fig. 2A). $\delta D_{nC_{31}}$ decreases from

-168‰ near the ancient shoreline to -195‰ more than 65 km upstream in the paleochannels, while $\delta D_{nC_{29}}$ ranges from -177‰ to -204‰ . Reconstructed $\Delta\delta D_{\text{precip}}$ is $>25\text{‰}$ and similar to $\Delta\delta D_{\text{kaolinite}}$ from similar site localities. Eocene sea-level δD_{precip} (-43‰ ; Mulch et al., 2006), in conjunction with our data, indicates that $\epsilon_{\text{apparent}}$ averages -125‰ , consistent with measured fractionations between modern angiosperm tree leaves and precipitation in humid environments (Chikaraishi and Naraoka, 2003).

We analyzed the distribution of soil tetraethers (GDGTs) in leaf-bearing sediments to constrain sea-level T ($^{\circ}\text{C}$) and ΔT across the mountain range. The T_{GDGT} at three sample localities closest to the Eocene ocean margin are $>22^{\circ}\text{C}$ and decrease along the upstream channel to $<15^{\circ}\text{C}$, leading to a maximum ΔT_{GDGT} of 16.5°C . While absolute temperature measures must be viewed carefully (Sinninghe Damsté et al., 2008), calculated Eocene temperatures are nearly identical to leaf-margin temperatures that we determined for several described Chalk Bluffs flora localities (MacGinitie, 1941) and an oxisol goethite temperature (Yapp, 2008), attesting to the veracity of these data (Fig. 2B; see the Data Repository). Comparison of early Eocene and modern MAT at individual paleofloral localities shows that early Eocene temperatures were at least $\sim 6\text{--}8^{\circ}\text{C}$ warmer than present across the length of the ancient Sierra Nevada.

$\Delta\delta D_{\text{precip}}$ can be related to range-scale paleotopography by establishing the pattern of isotopic distillation related to precipitation from a

vapor parcel during orographic lifting, adiabatic cooling, and rainout. Similarly, ΔT is related to paleochannel elevation by estimating adiabatic temperature lapse rates for the early Eocene. These are determined using a thermodynamic model that calculates the $\Delta\delta D_{\text{precip}}$ and ΔT as a function of elevation for a given sea-level temperature and relative humidity (RH) (Rowley et al., 2001; Rowley, 2007). Calculated temperature and isotope lapse rates are determined for three sea-level temperature inputs: (1) modern mean annual conditions at the base of the Sierra (sea-level MAT of 16°C and 75% RH), (2) sea-level MAT of 22°C and 82% RH (RH similar to modern tropical ocean areas with MAT of $20\text{--}25^{\circ}\text{C}$), and (3) a sea-level temperature equal to the highest measured T_{GDGT} (24.5°C and 82% RH) (Fig. 3). Early Eocene sediment data fall along the predicted ΔT and $\Delta\delta D$ contour for the high-temperature scenario (Fig. 3), and calculated lapse rates average $1.4\text{‰}/100\text{ m}$ for δD and $5.3^{\circ}\text{C}/\text{km}$ over the range of elevations from 0 to 3000 m. These are consistent with measured lapse rates in modern high-temperature, high-humidity environments and are used to calculate paleoelevations. Uncertainties for isotopic lapses and resulting paleoelevation estimates include errors associated with sea-level MAT ($\pm 4.1^{\circ}\text{C}$) and RH ($\pm 3.4\%$) inputs (Rowley, 2007).

Under the assumptions and limitations of the model to calculate paleoelevation based on changes in the isotopic composition of precipitation, reconstructed paleoelevations from

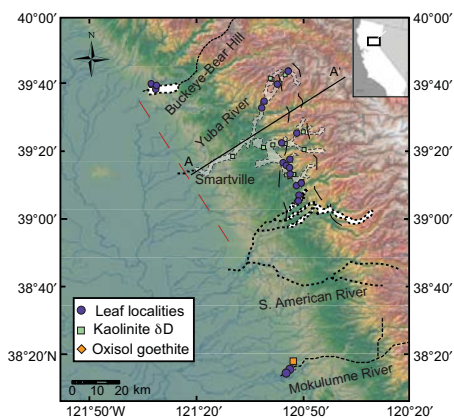


Figure 1. Sample location map of fossil leaf (blue circles) and kaolinite (green squares) localities in Eocene drainages (light blue shading) of paleorivers Buckeye–Bear Hill, American, Yuba, and Mokulumne. Locations are referenced relative to distance across range from Eocene shoreline marked by deltaic to marine lone Formation (red dashed line).

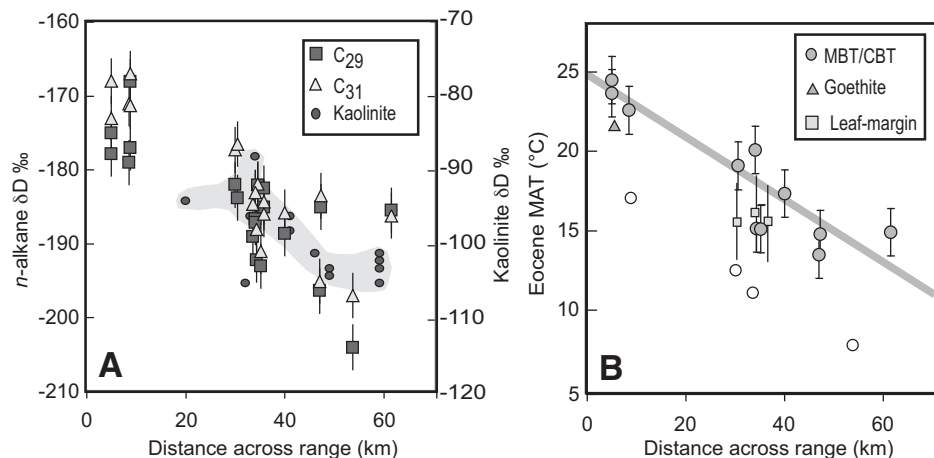


Figure 2. Data from fossil leaf localities across paleorange (line A–A'; see Fig. 1). **A:** $\delta D_{nC_{29}}$, nC_{31} . **B:** T_{GDGT} (mean annual temperature) as determined from the methylation index (MBT) and cyclization ratio (CBT) of branched glycerol dialkyl glycerol tetraethers. $\Delta\delta D_{n\text{-alkane}}$ equals that seen in associated kaolinites (Mulch et al., 2006) and reflects $\Delta\delta D_{\text{precip}}$ (precipitation) due to rainout during orographic lifting of airmasses across Eocene range. GDGT temperatures overlap leaf-margin temperatures and exceed modern mean annual temperatures (MAT) by more than 6°C . Low GDGT temperatures (open circles) could potentially reflect downstream transport from higher elevations. Shaded area highlights kaolinite data.

¹GSA Data Repository item 2010001, compound-specific stable isotope analyses and organic molecular temperature proxies, and Table DR1, is available online at www.geosociety.org/pubs/ft2010.htm, or on request from editing@geosociety.org or Documents Secretary, GSA, P.O. Box 9140, Boulder, CO 80301, USA.

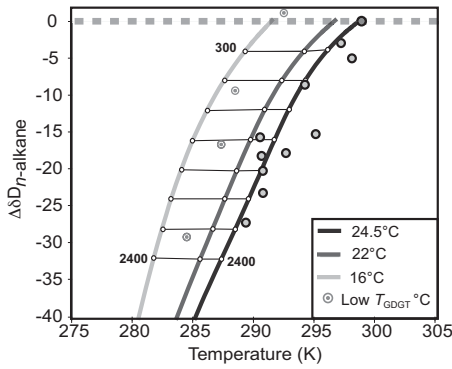


Figure 3. Calculated ΔT (temperature) and $\Delta\delta D_{\text{precip}}$ (precipitation) associated with orographic lifting of an airmass and associated rainout. Modern (16 °C) and two high-temperature scenarios are shown. Elevations associated with predicted isotope and temperature lapses are shown in white (circles). δD_{nC31} and T_{GDGT} (glycerol dialkyl glycerol tetraethers) are shown in black (circles). Anomalously low temperatures or enriched δD_{nC31} values fall off the high temperature line (bullseye).

$\Delta\delta D_{nC31}$ and modeled lapse rates range from sea level to >2200 m (+369/–754 m for the highest reconstructed elevations; Table DR1), topography similar to, or higher than, modern elevations. Paleoelevations reconstructed from ΔT in paleovalley sediments are comparable to reconstructed elevations from $\Delta\delta D_{\text{precip}}$, with the exception of several localities that are characterized by low GDGT temperatures, which produce high paleoelevation estimates (Fig. 4). We suspect that these low temperatures may reflect contribution of organics from higher elevation sites. Regardless, organic molecular temperatures and isotopic reconstructions produce equivalent range-scale and

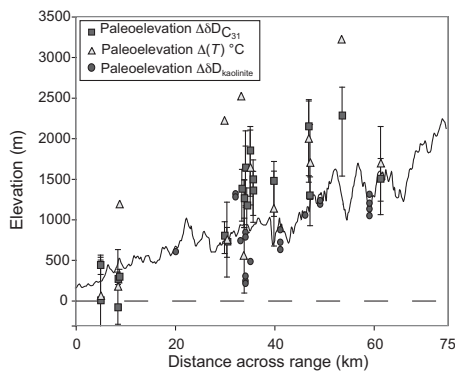


Figure 4. Reconstructed Eocene (52–49 Ma) paleoelevations of Sierra Nevada along line A-A' using ΔT_{GDGT} (glycerol dialkyl glycerol tetraethers) and $\Delta\delta D_{n\text{-alkane}}$. Errors reflect 2 σ uncertainty for modeled $\Delta\delta D_{\text{precip}}$ and ΔT with elevation in modern Sierra range. Dark line represents modern elevations along line A-A'.

channel paleoelevations that are equal to or higher than the modern. The small difference between atmospheric and ground-level proxy data (<400 m) suggests moderate to low relief in the early Eocene landscape.

Several factors can affect paleoelevation estimates of individual sites. Root uptake of stream water could reflect basin hypsometric δD rather than site δD_{precip} and thus record basin-weighted elevations. Leaves or biomarkers could be transported downstream with sediments. Both cases would produce overestimates of site elevation. Transport of leaves or leaf biomarkers is not likely a significant factor because virtually all extractable leaf-wax compounds are derived from cuticle within bulk sediments and downstream transport distances of intact leaves are generally short (<300 m; Cordova et al., 2008). The floodplain and in-filled meanders where Eocene leaves are preserved are ideal environments for organisms that produce branched tetraether compounds; however, it is possible that some component of measured GDGT biomarkers was transported from upstream areas. Four anomalously low GDGT temperatures could reflect contribution from eastern, high-elevation portions of the Eocene mountain range. We can be certain, however, that low temperatures do not reflect modern contamination, as analyses of modern Sierra Nevada soils in hillsides near exposed paleochannels provided no measurable GDGTs.

Organic molecular proxies record temperature and isotope gradients across the paleo-Sierra Nevada that can only be due to the presence of high-standing early Eocene topography. Ground-level (ΔT_{GDGT}) and range-scale ($\Delta\delta D_{n\text{-alkane}}$) paleoelevations are roughly equivalent and show that the major rivers of the Eocene Sierra Nevada drained a high-elevation (>2 km) subtropical landscape with temperatures at least 6–8 °C warmer than present. Paleoelevation estimates that reflect topography on different spatial scales suggest a moderate-low relief landscape; this is supported by low Cenozoic exhumation rates (Cecil et al., 2006) and intensely weathered Eocene laterites (MacGinitie, 1941) that reflect a prolonged soil-mantled landscape.

Higher than modern early Eocene elevations with moderate to low relief suggests that modern topography could have resulted from post-Paleocene reduction of range elevation through slow, prolonged weathering. Indeed, reconstructed paleoelevations from organic proxies (ca. 50 Ma) are higher at some sites (>250 m) than estimates from authigenic kaolinites that could have formed at any point between the deposition of Chalk Bluffs flora and overlying volcanic ashes (38.5 Ma; Yeend, 1974) and from similarly located volcanic glasses that date to the early Oligocene (31–28 Ma; Cassel et

al., 2009). Discrepancies between these proxies could result from higher temperature inputs for isotope and temperature lapse rate models for early Eocene leaf localities relative to younger kaolinite or Oligocene volcanic glasses, or show hypsometric lowering of paleocatchments. Isotope and temperature data from biomarkers, volcanic glasses, fossils, and clays indicate that the northern Sierra Nevada has remained a high-standing feature throughout most of the Cenozoic (Mulch et al., 2006, 2008; Crowley et al., 2008; Cassel et al., 2009). Apparent tilting of Miocene and younger paleochannels therefore likely reflects late Cenozoic increases in range relief in response to climatic change rather than increases in mean range elevations.

CONCLUSIONS

The δD of individual leaf waxes from ca. 52–49 Ma Chalk Bluffs flora, and soil-tetraether temperature measurements of leaf-bearing sediments, record atmospheric and ground-level paleoelevations that show the northern Sierra Nevada was a warm (>6–8 °C warmer), forested, high-elevation (>2 km) range with moderate to low relief at the peak of Eocene warming. These data, in conjunction with isotopic records of authigenic clays and volcanic glasses, suggest that the northern Sierra Nevada has been an enduring, high-elevation range throughout the Cenozoic. Modern topography likely reflects slow post-Paleocene reduction of overall northern Sierra Nevada range elevations and late Cenozoic increases in river incision that resulted in greater relief but did not significantly alter overall mean range elevations.

ACKNOWLEDGMENTS

We thank David Rowley for his model of isotopic evolution of precipitation during orographic ascent, and Howard Schorn, Daniel Peppe, and David Zinniker.

REFERENCES CITED

- Cassel, E.J., Graham, S.A., and Chamberlain, C.P., 2009, Cenozoic tectonic and topographic evolution of the northern Sierra Nevada, California, through stable isotope paleoaltimetry in volcanic glass: *Geology*, v. 37, p. 547–550, doi: 10.1130/G25572A.1.
- Cecil, M.R., Ducea, M.N., Reiners, P.W., and Chase, C.G., 2006, Cenozoic exhumation of the northern Sierra Nevada, California, from (U-Th)/He thermochronology: *Geological Society of America Bulletin*, v. 118, p. 1481–1488, doi: 10.1130/B25876.1.
- Chikaraishi, Y., and Naraoka, H., 2003, Compound-specific δD - $\delta^{13}C$ analyses of *n*-alkanes extracted from terrestrial and aquatic plants: *Phytochemistry*, v. 63, p. 361–371, doi: 10.1016/S0031-9422(02)00749-5.
- Cordova, J.M., Rosi-Marshall, E.J., Tank, J.L., and Lamberti, G.A., 2008, Coarse particulate organic matter transport in low-gradient streams of the Upper Peninsula of Michigan: *North American Benthic Society Journal*, v. 27, p. 760–771, doi: 10.1899/06-119.1.

- Crowley, B.E., Koch, P.L., and Davis, E.B., 2008, Stable isotope constraints on the elevation history of the Sierra Nevada: *Geological Society of America Bulletin*, v. 120, p. 588–598, doi: 10.1130/B26254.1.
- Ducea, M.N., and Saleeby, J.B., 1998, A case for delamination of the deep batholithic crust beneath the Sierra Nevada: *International Geology Review*, v. 40, p. 78–93, doi: 10.1080/00206819809465199.
- Garside, L.J., Henry, C.D., Faulds, J.E., and Hinz, N.H., 2005, The upper reaches of the Sierra Nevada auriferous gold channels, in Rhoden, H.N., et al., eds., *Window to the world: Reno, Geological Society of Nevada Symposium Proceedings*, p. 1–27.
- Hou, J., D'Andrea, J.D., and Huang, Y., 2008, Can sedimentary leaf waxes record D/H ratios of continental precipitation? Field, model, and experimental assessments: *Geochimica et Cosmochimica Acta*, v. 72, p. 3503–3517, doi: 10.1016/j.gca.2008.04.030.
- House, M.A., Wernicke, B., and Farley, K.A., 1998, Dating topography of the Sierra Nevada, California, using apatite (U-Th)/He ages: *Nature*, v. 396, p. 66–69, doi: 10.1038/23926.
- Huber, N.K., 1981, Amount and timing of late Cenozoic uplift and tilt of the central Sierra Nevada, California—Evidence from the upper San Joaquin River basin: U.S. Geological Survey Professional Paper 1197, 28 p.
- Ingraham, N.L., and Taylor, B.E., 1991, Light stable isotope systematics of large-scale hydrologic regimes in California and Nevada: *Water Resources Research*, v. 27, p. 77–90, doi: 10.1029/90WR01708.
- Jones, C.H., Farmer, G.L., and Unruh, J., 2004, Tectonics of Pliocene removal of lithosphere of the Sierra Nevada, California: *Geological Society of America Bulletin*, v. 116, p. 1408–1422, doi: 10.1130/B25397.1.
- Lindgren, W., 1911, *The Tertiary gravels of the Sierra Nevada of California*: U.S. Geological Survey Professional Paper 73, 226 p.
- MacGinitie, H.D., 1941, *A middle Eocene flora from the Central Sierra Nevada*: Contributions to Paleontology: Carnegie Institution of Washington Publication 534, 178 p.
- Meyer, H.W., 2007, A review of paleotemperature-lapse rate methods for estimating paleoelevation from fossil floras: *Reviews in Mineralogy and Geochemistry*, v. 66, p. 155–171, doi: 10.2138/rmg.2007.66.6.
- Mulch, A., Graham, S.A., and Chamberlain, C.P., 2006, Hydrogen isotopes in Eocene river gravels and paleoelevation of the Sierra Nevada: *Science*, v. 313, p. 87–89, doi: 10.1126/science.1125986.
- Mulch, A., Sarna-Wojcicki, A.M., Perkins, M.E., and Chamberlain, C.P., 2008, A Miocene to Pleistocene climate and elevation record of the Sierra Nevada (California): *National Academy of Science Proceedings*, v. 105, p. 6819–6824, doi: 10.1073/pnas.0708811105. 105.
- Poage, M.A., and Chamberlain, C.P., 2001, Empirical relationships between elevation and the stable isotope composition of precipitation and surface waters: Considerations for studies of paleoelevation change: *American Journal of Science*, v. 301, p. 1–15, doi: 10.2475/ajs.301.1.1.
- Poage, M.A., and Chamberlain, C.P., 2002, Stable isotopic evidence for a pre-middle Miocene rain shadow in the western Basin and Range: Implications for the paleotopography of the Sierra Nevada: *Tectonics*, v. 21, p. 1–16, doi: 10.1029/2001TC001303.
- Rowley, D.B., 2007, Stable isotope-based paleoaltimetry: Theory and validation: *Reviews in Mineralogy and Geochemistry*, v. 66, p. 23–52, doi: 10.2138/rmg.2007.66.2.
- Rowley, D.B., Pierrehumbert, R.T., and Currie, B.S., 2001, A new approach to stable isotope-based paleoaltimetry: implications for paleoaltimetry and paleohypsometry of the High Himalaya since the late Miocene: *Earth and Planetary Science Letters*, v. 5836, p. 1–17.
- Sachse, D., Radke, J., and Gleixner, G., 2006, δD values of individual n-alkanes from terrestrial plants along a climatic gradient—Implications for the sedimentary biomarker record: *Organic Geochemistry*, v. 37, p. 469–483, doi: 10.1016/j.orggeochem.2005.12.003.
- Saleeby, J., Ducea, M., and Clemens-Knott, D., 2003, Production and loss of high-density batholithic root, southern Sierra Nevada region: *Tectonics*, v. 22, 1064, doi: 10.1029/2002TC001374.
- Schimmelmann, A., Lewan, M.D., and Wintsch, R.P., 1999, D/H isotope ratios of kerogen, bitumen, oil, and water in hydrous pyrolysis of source rocks containing kerogen types I, II, IIS, and III: *Geochimica et Cosmochimica Acta*, v. 63, p. 3751–3766, doi: 10.1016/S0016-7037(99)00221-5.
- Sinninghe Damsté, J.S., Ossebar, J., Schouten, S., and Vershuren, D., 2008, Altitudinal shifts in the branched tetraether lipid distribution in soil from Mt. Kilimanjaro (Tanzania): Implications for the MBT/CBT continental palaeothermometer: *Organic Geochemistry*, v. 39, p. 1072–1076.
- Small, E.E., and Anderson, R.S., 1995, Geomorphically driven late Cenozoic rock uplift in the Sierra Nevada, California: *Science*, v. 270, p. 277–280, doi: 10.1126/science.270.5234.277.
- Smith, F.A., and Freeman, K.H., 2006, Influence of physiology and climate on δD of leaf wax n-alkanes from C3 and C4 grasses: *Geochimica et Cosmochimica Acta*, v. 70, p. 1172–1187, doi: 10.1016/j.gca.2005.11.006.
- Unruh, J.R., 1991, The uplift of the Sierra Nevada and implications for late Cenozoic epeirogeny in the western Cordillera: *Geological Society of America Bulletin*, v. 103, p. 1395–1404, doi: 10.1130/0016-7606(1991)103<1395:TUOTSN>2.3.CO;2.
- Wakabayashi, J., and Sawyer, T.L., 2001, Stream incision, tectonics, uplift, and evolution of topography of the Sierra Nevada, California: *Geology*, v. 109, p. 539–562, doi: 10.1086/321962.
- Weijers, J.W.H., Schouten, S., van den Donker, J.C., Hopmans, E.C., and Damsté, J.S.S., 2007a, Environmental controls on bacterial tetraether membrane lipid distribution in soils: *Geochimica et Cosmochimica Acta*, v. 71, p. 703–713, doi: 10.1016/j.gca.2006.10.003.
- Weijers, J.W.H., Schouten, S., Sluijs, A., Brinkhuis, H., and Sinninghe Damsté, J.S.S., 2007b, Warm Arctic continents during the Paleocene-Eocene thermal maximum: *Earth and Planetary Science Letters*, v. 261, p. 230–238, doi: 10.1016/j.epsl.2007.06.033.
- Wing, S.L., and Greenwood, D.R., 1993, Fossils and fossil climate: the case for equable continental interiors in the Eocene: *Royal Society of London Philosophical Transactions*, ser. B, v. 341, p. 243–252, doi: 10.1098/rstb.1993.0109.
- Yapp, C.J., 2008, $^{18}O/^{16}O$ and D/H in goethite from a North American oxisol of the Early Eocene Climatic Optimum: *Geochimica et Cosmochimica Acta*, v. 72, p. 5838–5851, doi: 10.1016/j.gca.2008.09.002.
- Yeend, W.E., 1974, Gold-bearing gravel of the ancestral Yuba River, Sierra Nevada, California: U.S. Geological Survey Professional Paper 772, 44 p.
- Zandt, G., Gilbert, H., Owens, T.J., Ducea, M., Saleeby, J., and Jones, C.H., 2004, Active foundering of a continental arc root beneath the southern Sierra Nevada in California: *Nature*, v. 431, p. 41–46, doi: 10.1038/nature02847.

Manuscript received 9 March 2009

Revised manuscript received 16 July 2009

Manuscript accepted 22 July 2009

Printed in USA